

Lawrence Berkeley National Laboratory

Recent Work

Title

WIRE CHAMBERS FOR CLINICAL IMAGING OF GAMMA-RAYS

Permalink

<https://escholarship.org/uc/item/6q80351w>

Authors

Kaufman, Leon
Perez-Mendez, Victor
Rindi, Alessandro
et al.

Publication Date

1970-06-01

Submitted to Physics in
Medicine and Biology

UCRL-19772
Preprint

c.2

RECEIVED
LAWRENCE
RADIATION LABORATORY

AUG 19 1970

LIBRARY AND
DOCUMENTS SECTION

WIRE CHAMBERS FOR CLINICAL
IMAGING OF GAMMA-RAYS

Leon Kaufman, Victor Perez-Mendez, Alessandro Rindi,
Johnie M. Sperinde, and Harold A. Wollenberg

June 1970

AEC Contract No. W-7405-eng-48

TWO-WEEK LOAN COPY

*This is a Library Circulating Copy
which may be borrowed for two weeks.
For a personal retention copy, call
Tech. Info. Division, Ext. 5545*

48 LAWRENCE RADIATION LABORATORY
UNIVERSITY of CALIFORNIA BERKELEY

UCRL-19772
c.2

DISCLAIMER

This document was prepared as an account of work sponsored by the United States Government. While this document is believed to contain correct information, neither the United States Government nor any agency thereof, nor the Regents of the University of California, nor any of their employees, makes any warranty, express or implied, or assumes any legal responsibility for the accuracy, completeness, or usefulness of any information, apparatus, product, or process disclosed, or represents that its use would not infringe privately owned rights. Reference herein to any specific commercial product, process, or service by its trade name, trademark, manufacturer, or otherwise, does not necessarily constitute or imply its endorsement, recommendation, or favoring by the United States Government or any agency thereof, or the Regents of the University of California. The views and opinions of authors expressed herein do not necessarily state or reflect those of the United States Government or any agency thereof or the Regents of the University of California.

WIRE CHAMBERS FOR CLINICAL
IMAGING OF GAMMA-RAYS*

LEON KAUFMAN, Ph.D.

University of California, San Francisco, California

VICTOR PEREZ-MENDEZ, Ph.D.

University of California, San Francisco, California
and Lawrence Radiation Laboratory, Berkeley, California

and

ALESSANDRO RINDI, Ph.D.

JOHNNIE M. SPERINDE, B.A.

HAROLD A. WOLLENBERG, B.S.

Lawrence Radiation Laboratory, Berkeley, California

ABSTRACT

Spark chambers with digitized readouts offer distinct advantages in spatial resolution and coverage over other gamma-ray imaging devices. While these chambers usually require external logic signals for triggering, in this paper we describe a method that provides self-triggering spark chambers. We also describe initial tests of a 45 X 45 cm spark chamber with ^{60}Co and ^{198}Au samples. Future developments are mentioned.

1. Introduction

The widespread use of gamma-ray-emitting radioisotopes has become a powerful tool in clinical diagnosis and in human and animal physiology studies. While present devices for the spatial imaging of isotope distributions tend to be limited both in resolution and area coverage, wire spark chambers with electronic readout afford compact instruments that are able to cover large areas with high resolution and supply quantitative information at low cost.

2. The Spark Chamber

Spark chambers in their simplest form consist of two parallel conducting plates (of areas reaching many square meters) separated by a gap of 1 cm typical size. The volume between the gaps is filled with a noble gas and a quenching gas such as alcohol.

If a high-voltage pulse is applied during or shortly after the passage of an ionizing particle through the active volume of the chamber, a spark will develop. Typical sparking voltages are of the order of a few kilovolts per centimeter.

If the metal plates in the spark chamber are replaced by wire planes, and a suitable method to sample the wires is used, coordinates can be read out electronically. In our chambers the wires in one plane run at 90 deg to the wires in the other so that X and Y coordinates can be obtained (fig. 1), and Mylar windows are used to seal the chamber.

The sampling system consists of a magnetostrictive (Perez-Mendez and Pfab 1965) wire (typically a ferromagnetic alloy) placed close to, but not in contact with, the chamber wires. The particular wire (or wires) carrying current to the spark are surrounded by a rapidly changing magnetic field. The properties of magnetostrictive materials are such that their length varies with magnetic field. The fast increase and decrease of field around the sensor wire produces a rapid contraction and relaxation in that wire. This disturbance travels down the line with acoustic speeds (about 5000 m/sec). A detector consisting of a pickup coil and amplifier produces a signal that is processed by the technique of differentiation and zero crossing so that the center of gravity of the spark current can be determined. The steps involved in this process can be seen in fig. 2. The signal is timed by 20 MHz scalars; the number of sparks that can

be detected depends on the number of scalers used. To make the system independent of the positioning of the magnetostrictive line and of conditions that affect the speed of sound in that line, we connect the first and last wires in each plane through a resistor-capacitor chain. In this way, a current flows through these wires each time the chamber is pulsed, and two marker or "fiducial" pulses are obtained on the line. The first fiducial turns the timing clocks on, the spark turns one clock off and a second spark or fiducial turns the other clock off. In the latter case we obtain an absolute normalization of distances along the line. The schematics of the electronics can be seen in fig. 2.

For a wire-to-wire separation of 1 mm, we obtain location accuracies of ± 0.33 mm, this being due to the fact that the current splits proportionately to the distances from the track to the two wires that straddle it. These spark chambers produce data that can be stored on tape or analyzed on-line, and have been in use for the last five years (Perez-Mendez, Devlin, Solomon, and Droege 1967).

In many experimental situations the range and energy of the detected particles is sufficiently large so that the events are selected by a triggering signal derived from scintillation counters placed strategically around the spark chambers to form an appropriate coincidence for the event. Such a triggering system is less effective in dealing with γ rays or other neutral particles whose presence is detected by secondary charged particles produced in converters placed in or around the wire planes (fig. 3), and becomes especially inefficient when dealing with low-energy γ rays from radioactive sources, or X-rays, where the range of the secondary electrons is small enough so that they often do not emerge from a single gap.

Since our interest is in using wire chambers for medical diagnostic purposes--the localization of γ -emitting radioactive isotopes with energies ranging from tens of keV to a few MeV--we have investigated the characteristics of the signals produced by low-energy charged particles in the pre-avalanche region in the wire chamber and the sparking characteristics of the chamber itself when triggered by these signals.

A basic feature of our scheme is that we preserve the ability to read out spark coordinates electrically by the magnetostrictive delay-line methods so that we retain the ease of handling and computing large numbers of events; in this respect we differ from other work in which some form of self-triggering methods are used and the sparks are subsequently photographed (Roux, Gaucher, LeLoup, Morucci and Lansart 1968).

3. Experimental

The spark chamber used to test the properties of gas-multiplication triggering has an active area of 20 cm X 20 cm and a capacity of 140 pF (Rindi, Sperinde, Kaufman and Perez-Mendez 1968). It consists of three planes, the central one made up by stringing 0.08 mm steel wires 1.5 mm apart over a lucite frame. The outside planes are of copper-etched Mylar, 1 mm wide, 1 mm apart. The distance between the planes is 1 cm in each case, and magnetostrictive readout is possible from the two outside planes. For operation, the chamber is filled at atmospheric pressure with a 90% Ne - 10% He gas mixture saturated at room temperature with ethyl alcohol (~ 50 mm Hg).

Figure 4 shows the circuit used for particle detection and spark triggering. The outer electrodes are grounded and a positive high voltage was applied to the central one. A 22 M Ω resistor is used to limit the current

available to the chamber and prevent a continuous discharge. The resistor also determines the recovery time of the chamber for detection of particles after sparking, since it limits the recharging rate of the chamber.

The proportional pulses are collected from the high-voltage electrode through a 100 pF capacitor into a voltage-sensitive preamplifier with an input impedance of 10 k Ω . The preamplifier has a gain of ~ 20 and its pulses are fed into a variable-gain linear amplifier. The preamplifier is protected during sparking by a simple back-to-back diode system with a 1 k Ω resistor to limit the current through the diodes. The spark chamber is decoupled by a series gap from the capacitor in the high-voltage pulsing system.

When the chamber is operated with the gas mixture previously described ~ 0.25 mv pulses are obtained for an applied voltage of 3900 v; this corresponds to a gas amplification of approximately 6000. The shape of this pulse can be seen in fig. 5.

The detection efficiency of the chamber was tested by placing it between two scintillation detectors and counting simultaneously double (between the scintillators only) and triple coincidences. The results, as a function of applied dc voltage, can be seen in fig. 6.

Using a variable threshold discriminator set to trigger at 10% of the height of the average pulses, we find that it fires about 0.4 μ sec after passage of the particle through the chamber. Since no appreciable losses in sparking efficiency are seen for times up to 0.5 μ sec after passage of the particle (see fig. 7), the delay can be tolerated. The triggering jitter time is less than 0.3 μ sec (see fig. 8). We observed also that the operation of the chamber is moderately insensitive to the rise time of the high-voltage pulse and that rise times of ~ 50 nsec do not cause any loss in efficiency.

We have also measured the rekindling time of this chamber (time during which a spark will be formed along the path of a previous spark, i.e., the number of double sparks on the same track as a function of the delay time between the sparks). This is shown in fig. 9 for a particular set of parameters.

All these characteristics of the chamber (memory time, jitter time, rekindling time, proportional pulses shape, etc.) are functions of many parameters, of which we list the most important: the type of gas in the chamber, the type and concentration of quenching agent (ethanol, methanol, etc.), the high voltage used for the proportional pulses which influences the sparking conditions, and the energy in the sparks. These parameters can be optimized for the particular requirements needed from the chambers.

4. A Gamma-Ray Scanner for Clinical Uses

Magnetostrictive readout spark chambers coupled to converters, i.e., lead plates, offer distinct advantages over present systems for the imaging of γ -ray emitting radionuclides: 1 mm or better accuracy of location, large area for whole body scanning, and low cost. Such a system with an active area of 45 X 45 cm is presently being used by us (Kaufman, Perez-Mendez, and Wollenberg 1968), and the schematics are shown in fig. 10.

When imaging single γ -ray-emitting nuclei, a collimator placed between the source and detector is commonly used. For all practical applications, the resolution of the system is given by the hole size and configuration of the collimator. In our work the chamber is triggered on all counts in the scintillator except the ones blocked by the cosmic-ray anticoincidence counter. Not all triggers correspond to real events since an appreciable number of γ rays will convert in the scintillator itself, giving rise to false triggers, and conversely, not all electrons reaching the chamber give rise to a trigger signal.

It is in this type of application that full advantages of gas-multiplication-triggered spark chambers are realized, since they allow for detection of particles that would not register otherwise, and an increase in detection efficiency produces a directly proportional increase in sensitivity. It is generally the case that data collection is sensitivity-limited rather than spark chamber recovery-time-limited, so that the advantage of gas-multiplication triggering is that it allows for an increase of data collection rates through improved sensitivity.

We have performed computer simulations of collimators, and found that for constant resolution, the acceptance (fraction of γ rays being collimated) increases with increasing thickness, since the density of holes can be increased. We have built and tested with ⁶⁰Co sources, two 15 cm thick lead collimators with 5 mm diameter holes. The first, which has 5 mm septa, was found to give a granular image, the resolution of the detector making it easy to see each individual hole. The second collimator has 3 mm septa, and individual holes are still discernible, although to a lesser extent than in the previous case. We feel then that 1-2 mm septa will be adequate for 5 mm holes. Experimental resolution curves obtained with the second collimator are shown in fig. 11. From these preliminary results, we conclude that for applications where high resolution is desired, collimators with holes as small as 1 mm could be used.

Full advantage of the high resolution and large scanned areas that spark chambers make available can only be realized through the use of computers. Pictures can be obtained on-line by the use of an ADC (Analogue-to-digital converter) unit, which converts the digitized information into voltages that are applied to the X and Y inputs of a cathode ray tube, with a Z-intensify signal applied

simultaneously. While the pictures are useful, computer analysis allows for background subtraction, selective contrast enhancement, quantitative output, high resolution, etc. Figures 12 through 17 show pictures and computer outputs of various phantoms. These were taken with the 45 X 45 cm single gap spark chamber and a 15 cm thick, 5 mm diameter hole, 3 mm septa, Pb collimator. It can be seen that simple schemes of background subtraction yield pictures that are extremely clean, thus showing that the system more than makes up for the lack of pulse height discrimination when advantage is taken of the high location accuracy of the chambers. We are presently developing simple methods for information display and analysis. Since the possible processing schemes are numerous, each user will have a large variety of choices to suit his particular needs.

5. Future Directions

We are presently studying (Rindi, Perez-Mendez, and Wallace 1970) a scheme by which we can retain the simplicity of the delay-line readout method and at the same time acquire the capability of obtaining high event rates ($>10^5$ events/sec).

In spark chambers, limits on the data rate are imposed by the need to wait until the ion pairs released by the spark have either recombined or been removed by clearing fields and/or quenching gases. The recent development of wire chambers in which the proportional pulse is used for spatial location (Charpak, Bouclier, Bressani, Favier and Zupancic 1968) allows for considerably increased data rates. For these chambers one of the main difficulties is that the presently used readout methods, which involve the use of individual amplifiers at each wire, are both tedious to construct and somewhat costly (Charpak et al; and Amato and Petrucci 1968). In order to retain the simplicity of a delay-line

readout method, together with the fast event rate which these proportional wire chambers are capable of recording, we have investigated the use of ferrite-loaded and air core delay cables for this purpose. These cables have high coupling efficiencies, with sufficient delay to enable present-day electronics to record track positions to an accuracy comparable to the wire spacing, in a time that does not exceed the storage time of the event. We have shown (Rindi et al) that multiwire proportional chambers could be successfully operated with delay cables, thus attaining the aim of combining high data rates and the simplicity of delay-line readouts. We expect to combine these new developments into a more advanced γ -ray imaging system.

REFERENCES

* This work was done under the auspices of the U.S. Atomic Energy Commission

Amato, G., and Petrucci, G., 1968, CERN Report CERN-68-33.

Charpak, G., Bouclier, R., Bressani, T., Favier, J., and Zupancic, C., 1968, Nucl. Instr. Methods, 62, 262; 1968, 65, 217.

Kaufman, L., Perez-Mendez, V., and Wollenberg, H., June 1968, Applications of Digitized Readout Spark Chambers to Clinical Uses, Lawrence Rad. Lab. Report UCID-3184.

Perez-Mendez, V., Devlin, T. J., Solomon, J., and Droege, T. F., 1967, Nucl. Instr. Methods, 46, 197.

Perez-Mendez, V. and Pfab, J. M., 1965, Nucl. Instr. Methods, 33, 141.

Rindi, A., Sperinde, J. M., Kaufman L., and Perez-Mendez, V., October 1968, Ionization-Triggered Wire Chambers with Magnetostrictive Readout, Lawrence Rad. Lab. Report UCID-3271.

Rindi, A., Perez-Mendez, V., and Wallace, R. I., 1970, Nucl. Instr. Methods, 77, 325.

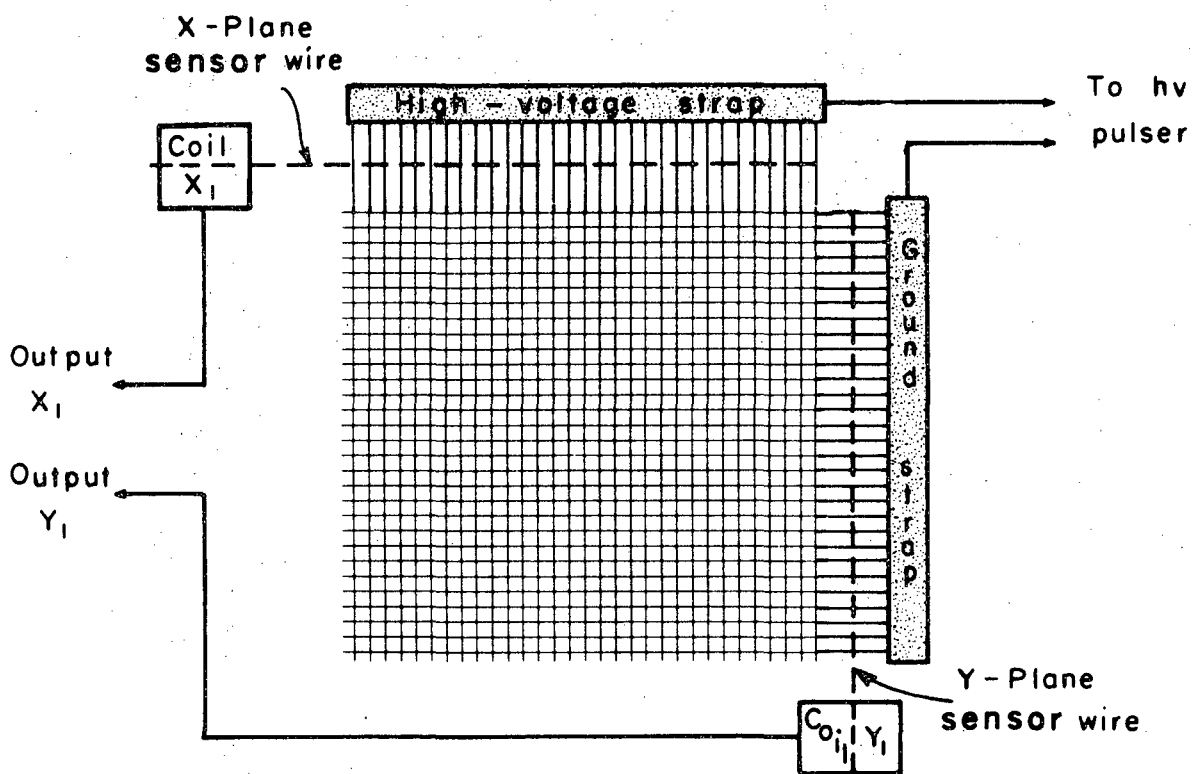
Roux, G., Gaucher, J. C., LeLoup, J., Morucci, J. P., and Lansiert, A., 1968, I.E.E.E. Trans. Nuc. Sci. NS-15, 67.

FIGURE CAPTIONS

- Fig. 1. Schematics of a magnetostrictive readout wire spark chamber.
- Fig. 2. Schematics of the magnetostrictive signal processing system.
- Fig. 3. Scintillation trigger for the detection of low-energy gamma rays. The primary radiation produces an electron either in the lead or within the chamber. Detection of this electron by the scintillator gives rise to a logic signal that can be used to trigger the spark chamber.
- Fig. 4. Setup for gas-multiplication triggering of a spark chamber.
- Fig. 5. Pulse shapes obtained from the linear amplifier in fig. 4.
- Fig. 6. Detection efficiency "e" of the gas-multiplication-triggered spark chamber as a function of applied dc voltage.
- Fig. 7. Sparking efficiency as a function of trigger delay. The gas is 90% Ne-10% He. The delay time is measured after particle detection by the chamber. Curve A has 3400 v dc and 50 mm Hg of ethanol as the quenching gas; curve B has 4000 v dc and 215 mm Hg of methanol.
- Fig. 8. Number of counts as a function of the time between the passage of an ionizing particle through the chamber and its detection. Discrimination was set at 10% of the average height of the proportional pulses.
- Fig. 9. Rekindling of old sparks as a function of time between high-voltage (hv) pulses. Pulsing was done by discharging a 500 pF capacitor at 9 kv. The chamber was flushed at atmospheric pressure with a 90% Ne - 10 He gas mixture saturated with ethyl alcohol (~ 50 mm Hg).
- Fig. 10. Schematics of the gamma imaging system in use.
- Fig. 11. System response to a 50 μ Ci ⁶⁰Co point source for a lead collimator of 5 mm diameter holes, 3 mm septa, and 15 cm thick. Shown in 11a: 1 mm bins; 11b: 5 mm bins.
- Fig. 12. 0.5 mm diameter, 62.5 mm long wire with 50 μ Ci of ⁶⁰Co. Computer reconstruction of data of the 45 X 45 cm spark chamber. Lead collimator of 5 mm diameter holes, 3 mm septa, and 15 cm thick. 25 000 points. Scale in centimeters.
- Fig. 13. Expanded view of the area of interest in fig. 12. Scale in centimeters.
- Fig. 14. Same as fig. 13, with 20% background subtraction. 1200 points.
- Fig. 15. Rat's liver and spleen, labeled with 170 μ Ci of ¹⁹⁸Au, as seen with the Anger camera. Lead collimator of 7 mm diameter holes, 5 mm septa, and 76 mm thick. 1 000 000 counts.

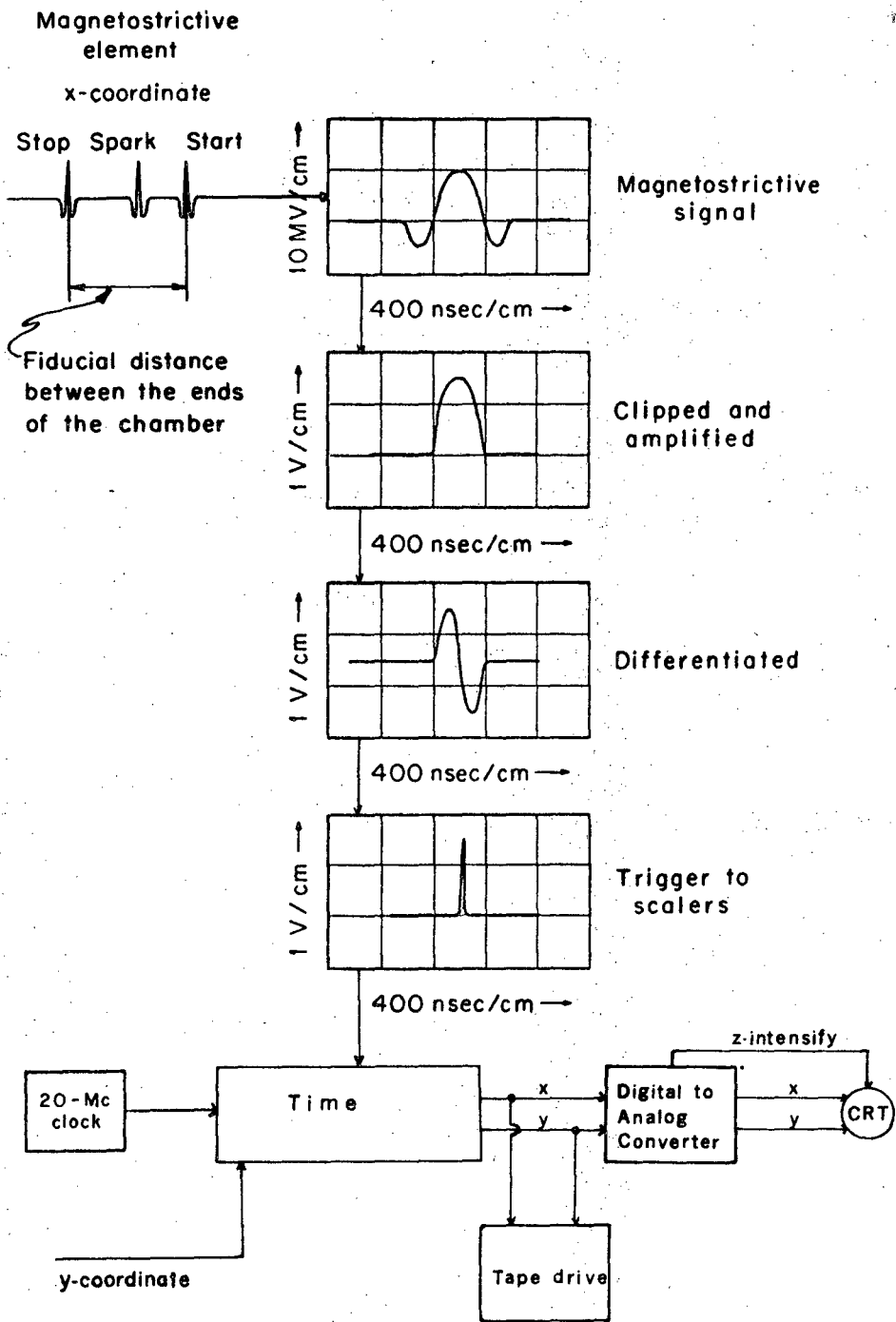
Fig. 16. Rat's liver and spleen, labeled with 170 μ Ci of ^{198}Au ; computer reconstruction of data of the 45 X 45 cm spark chamber, with 10% background subtraction. Lead collimator of 7 mm diameter holes, 5 mm septa, and 76 mm thick. 20 000 points. Scale in centimeters.

Fig. 17. Same as Fig. 16 but with 20% background subtraction.



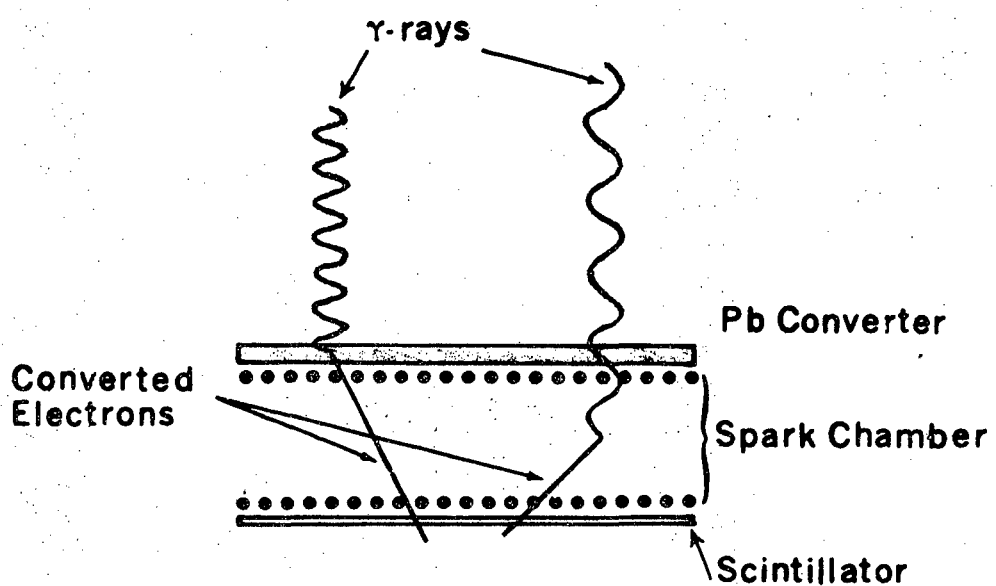
XBL 706-1074

Fig. 1



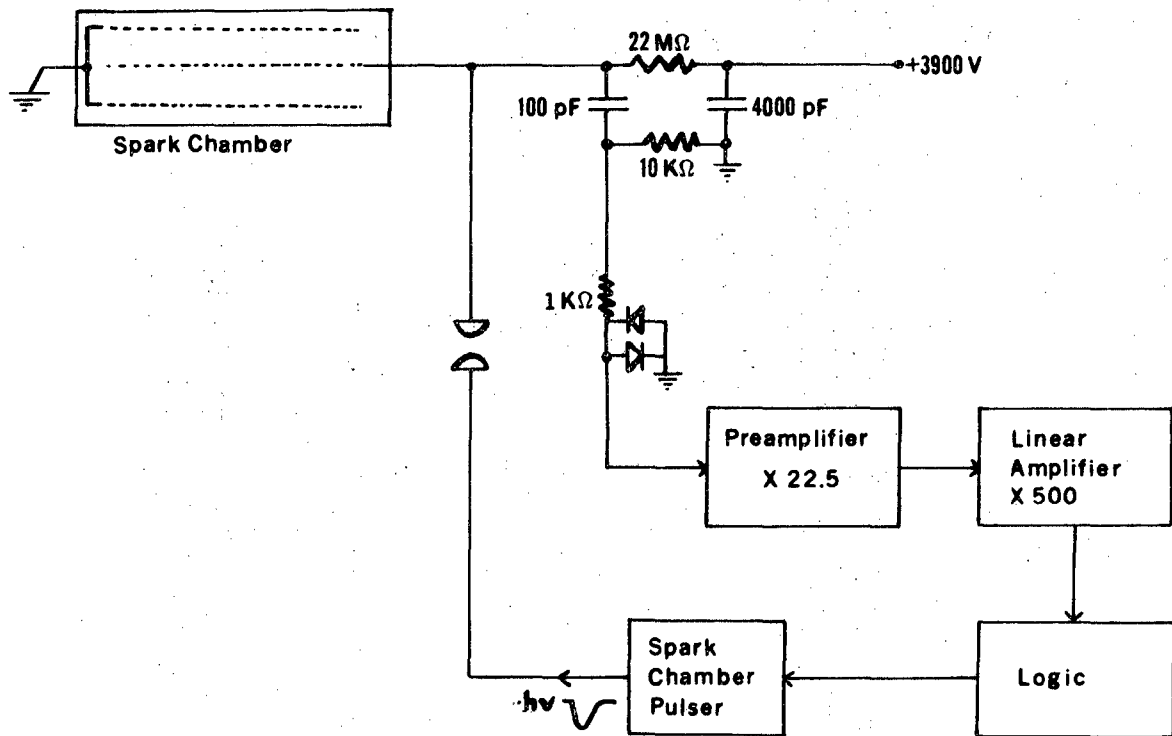
XBL706-3051

Fig. 2



XBL 706-1159

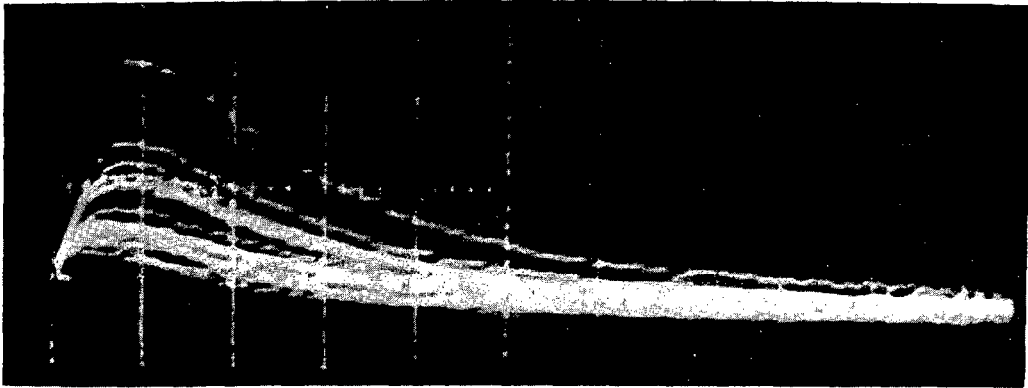
Fig. 3



XBL 706-1160

Fig. 4

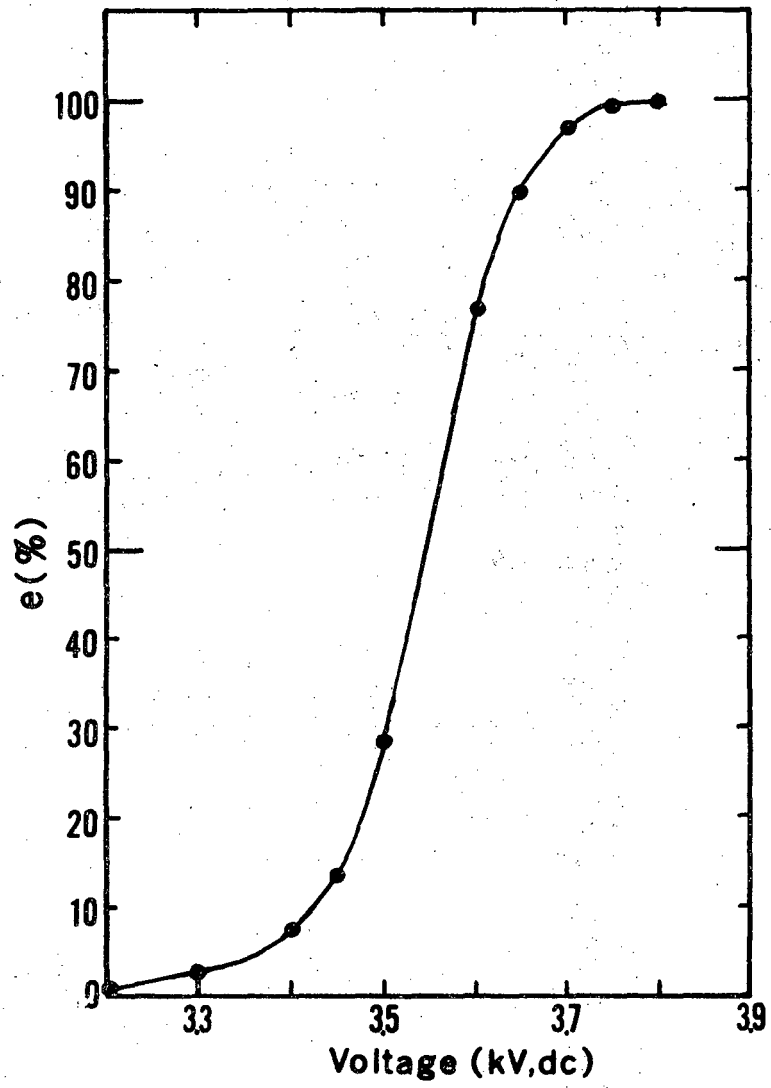
2V/cm



1 μ sec/cm

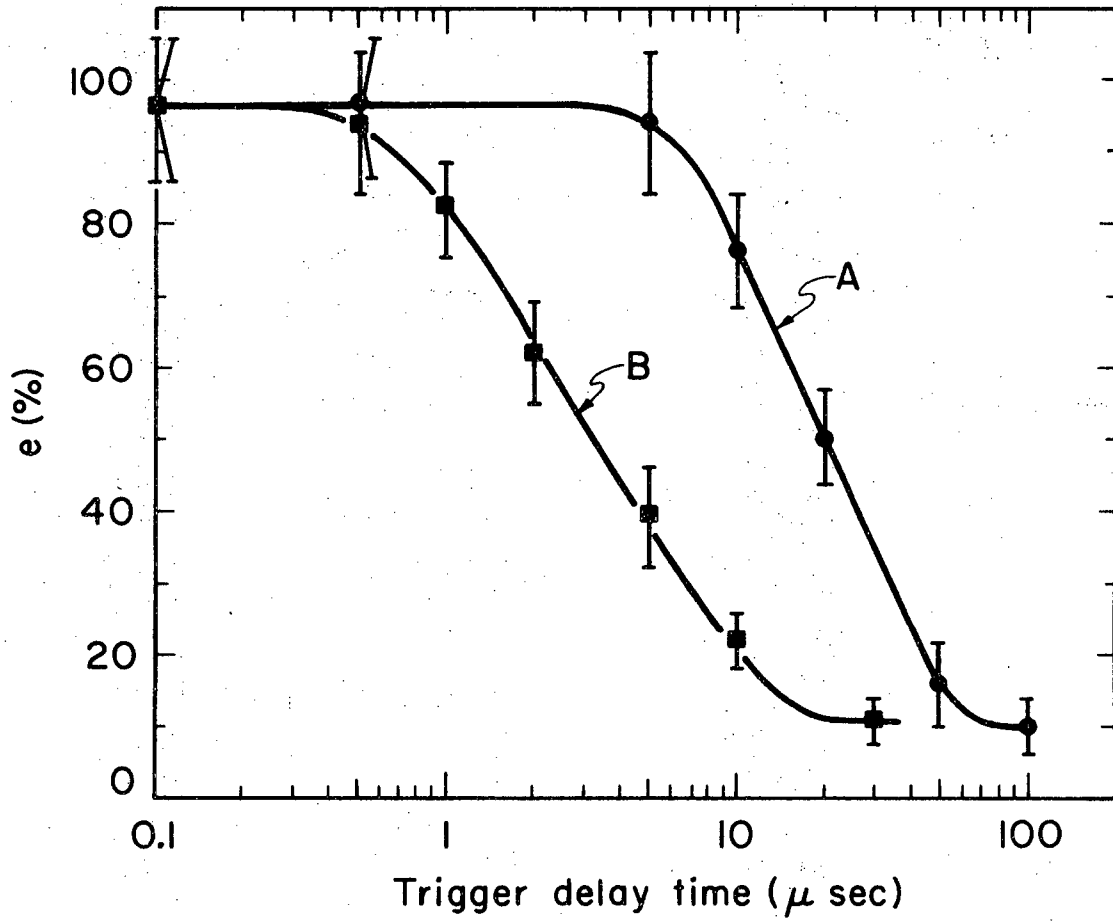
XBB 706-2701

Fig. 5



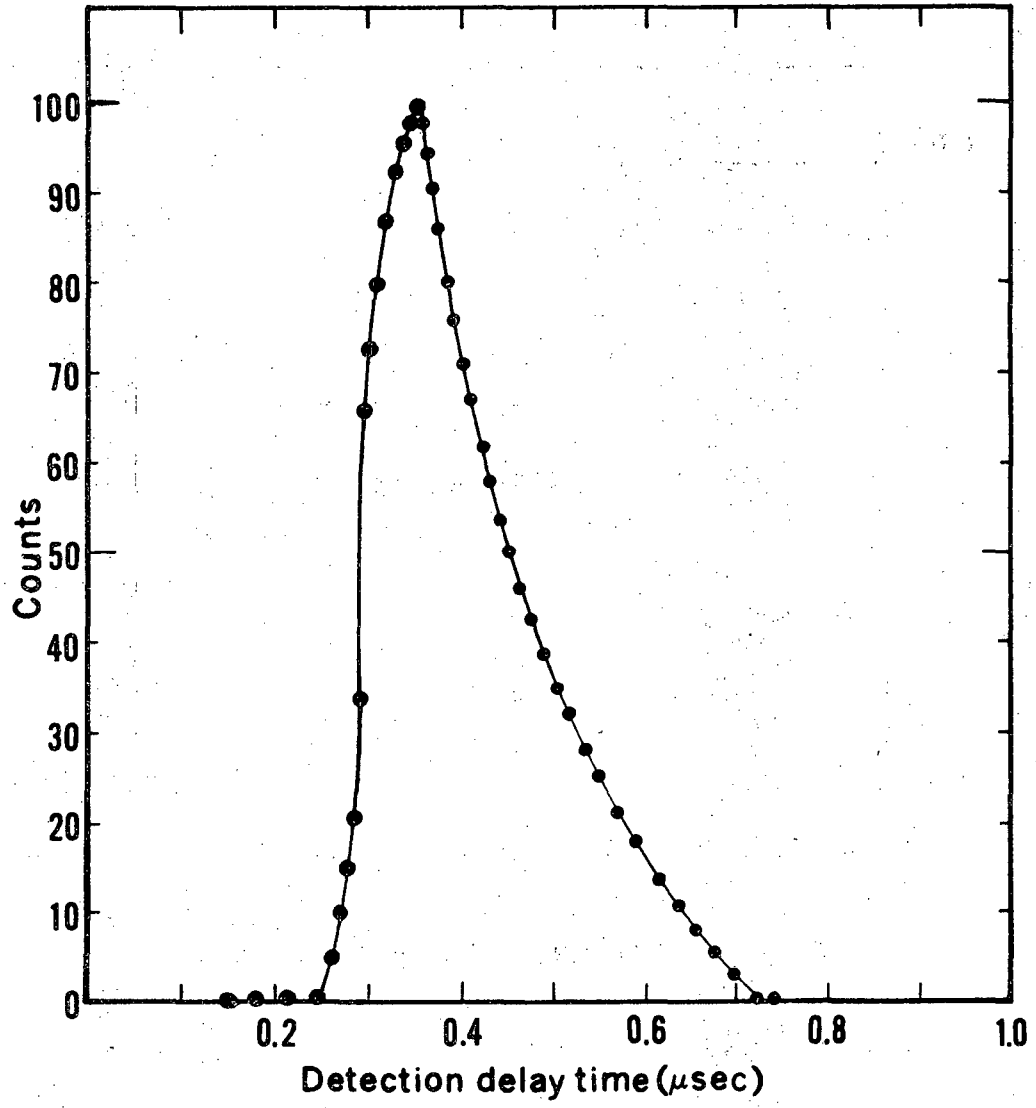
XBL706-3053

Fig. 6



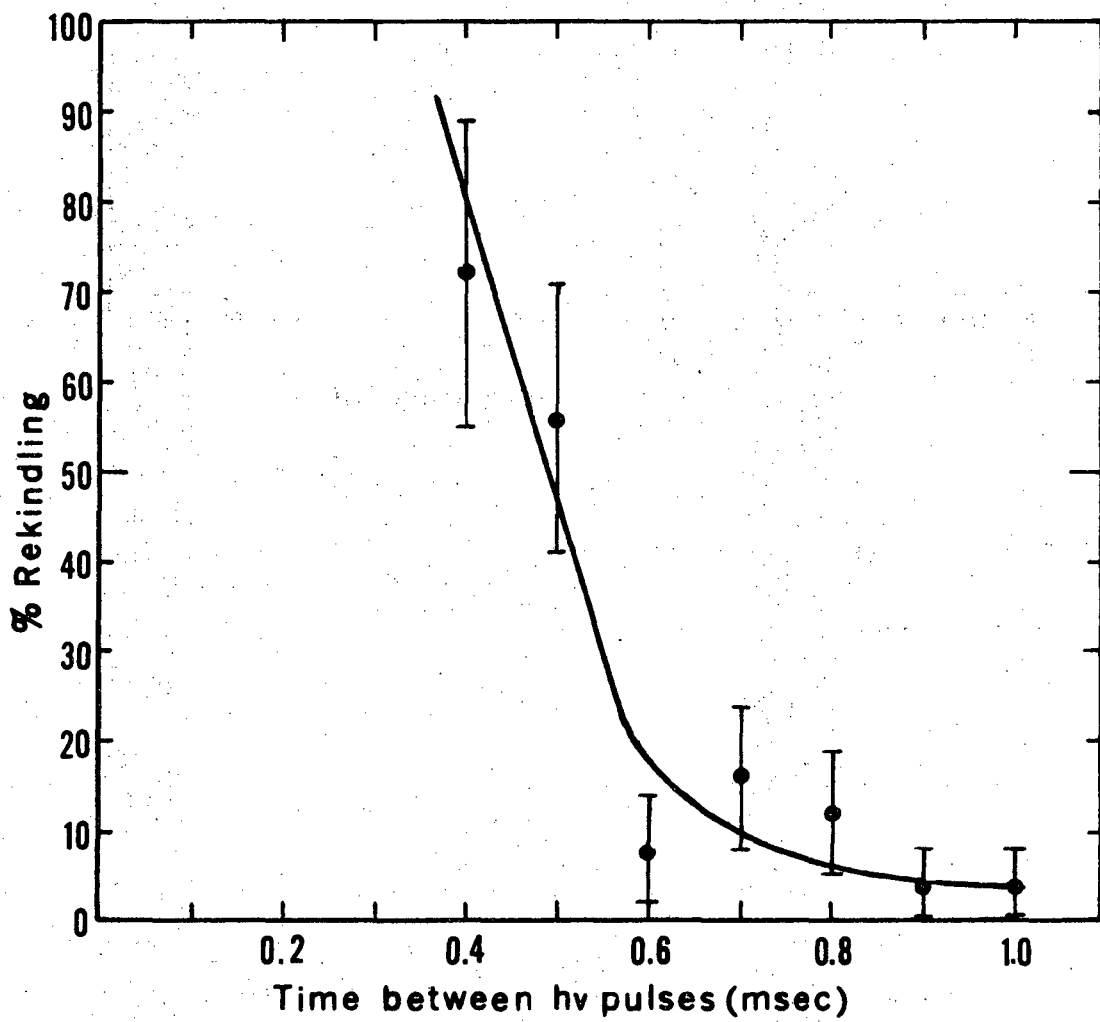
XBL706-3055

Fig. 7



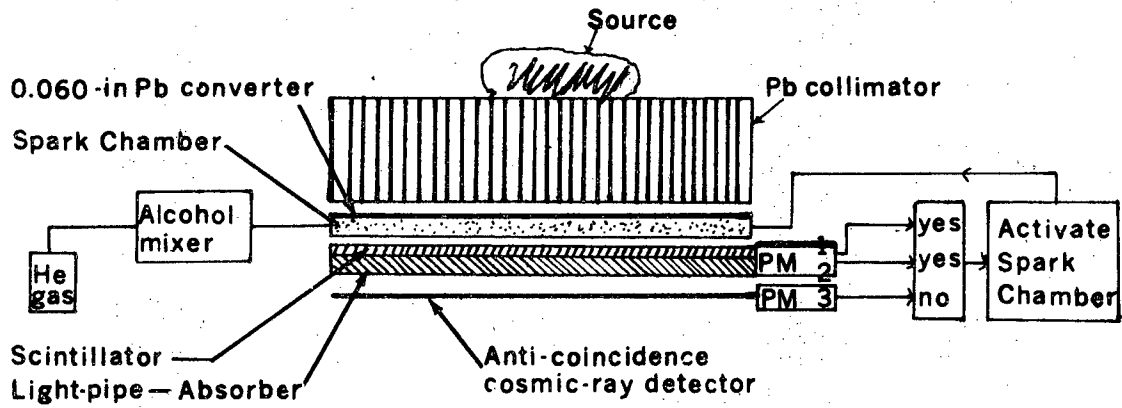
XBL706-3056

Fig. 8



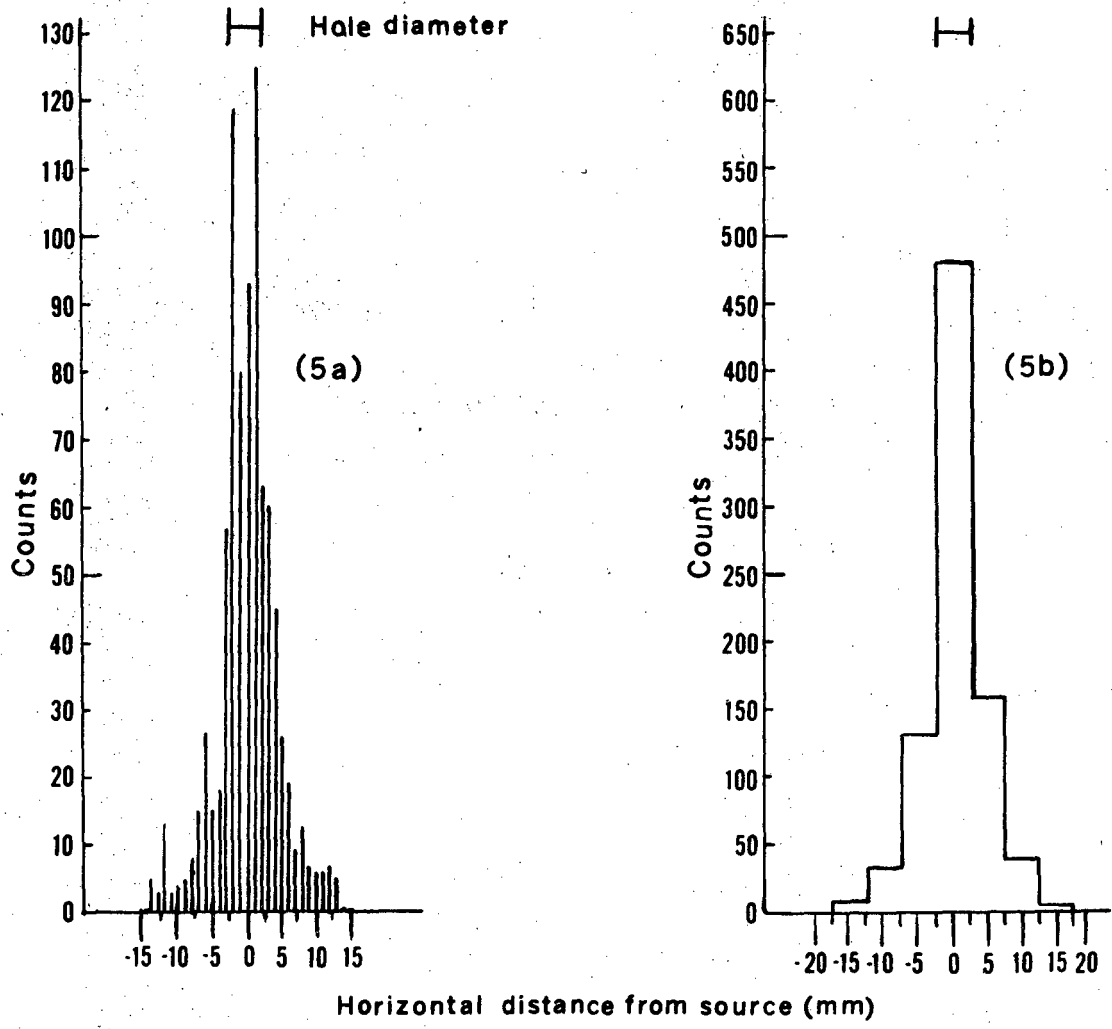
XBL706-3054

Fig. 9



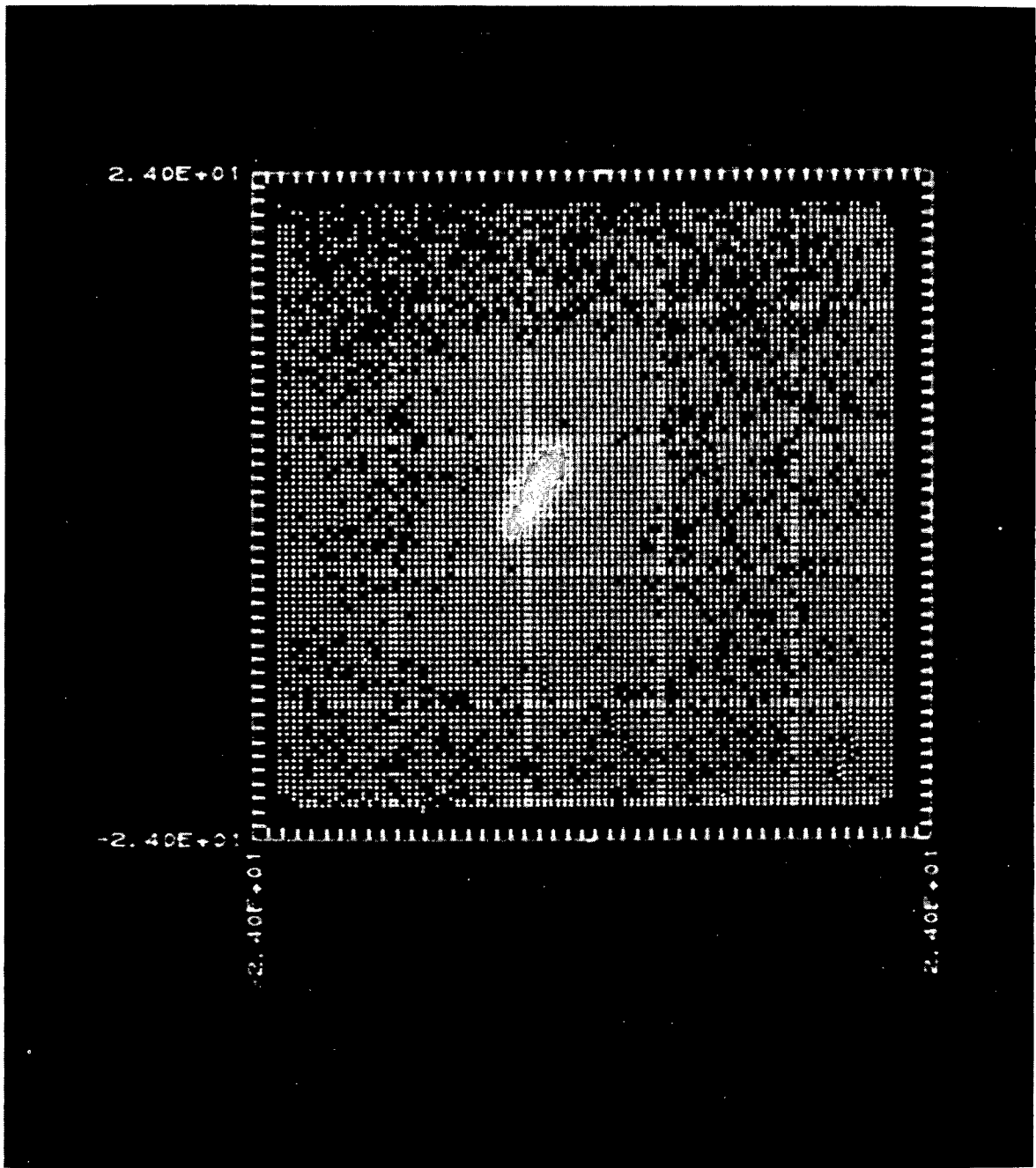
XBL 706-1161

Fig. 10



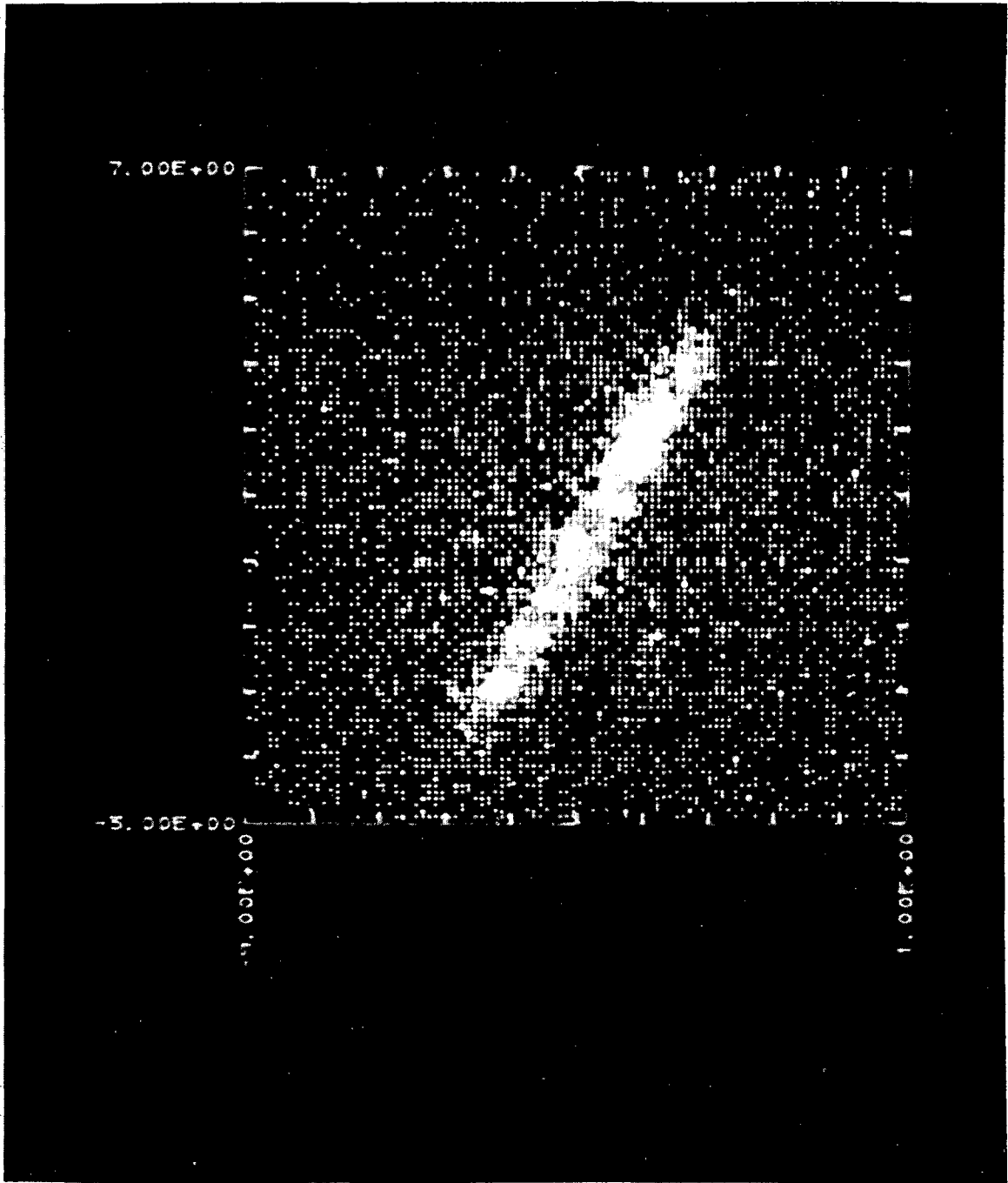
XBL706-3052

Fig. 11



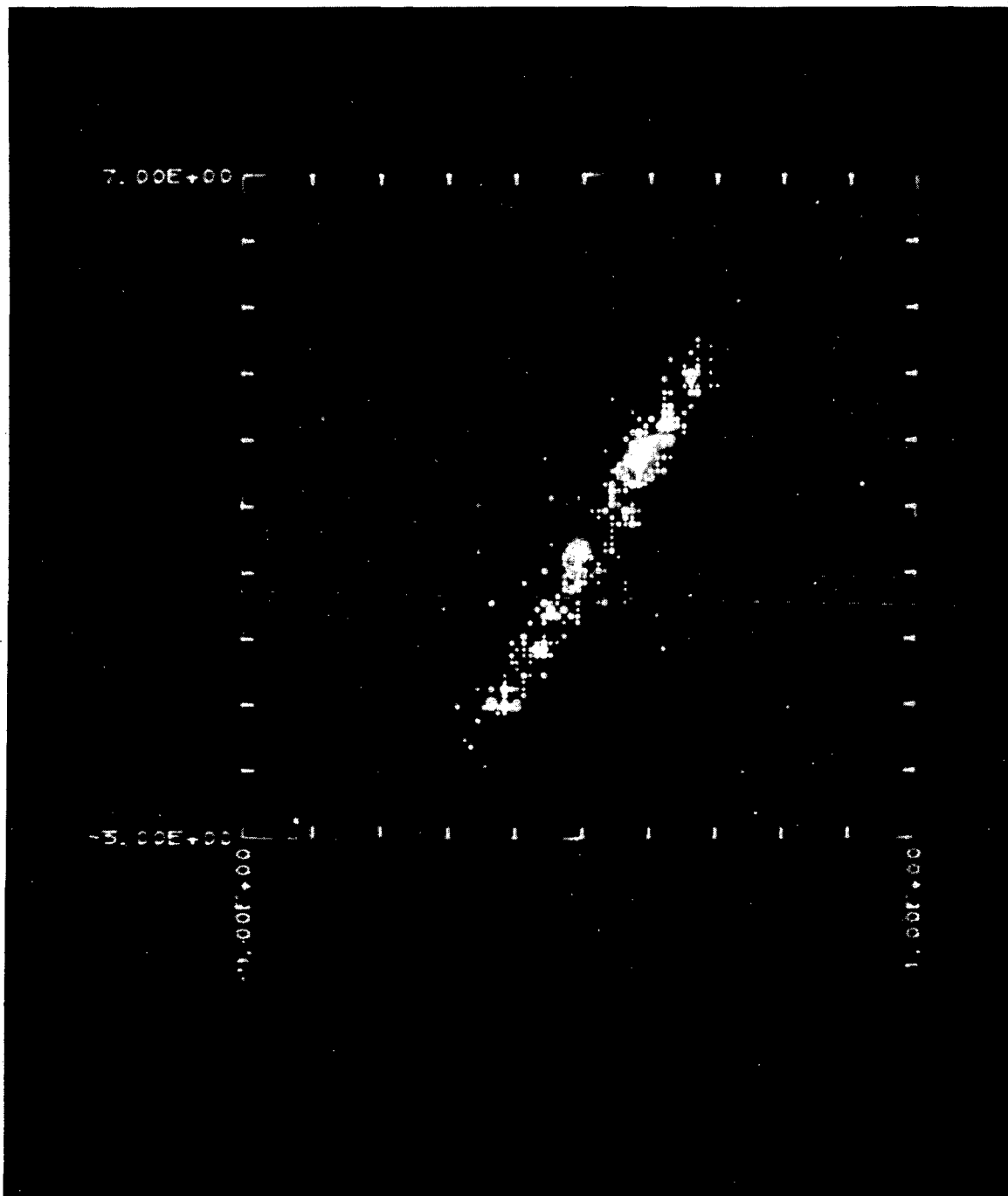
XBB 686-3752

Fig. 12



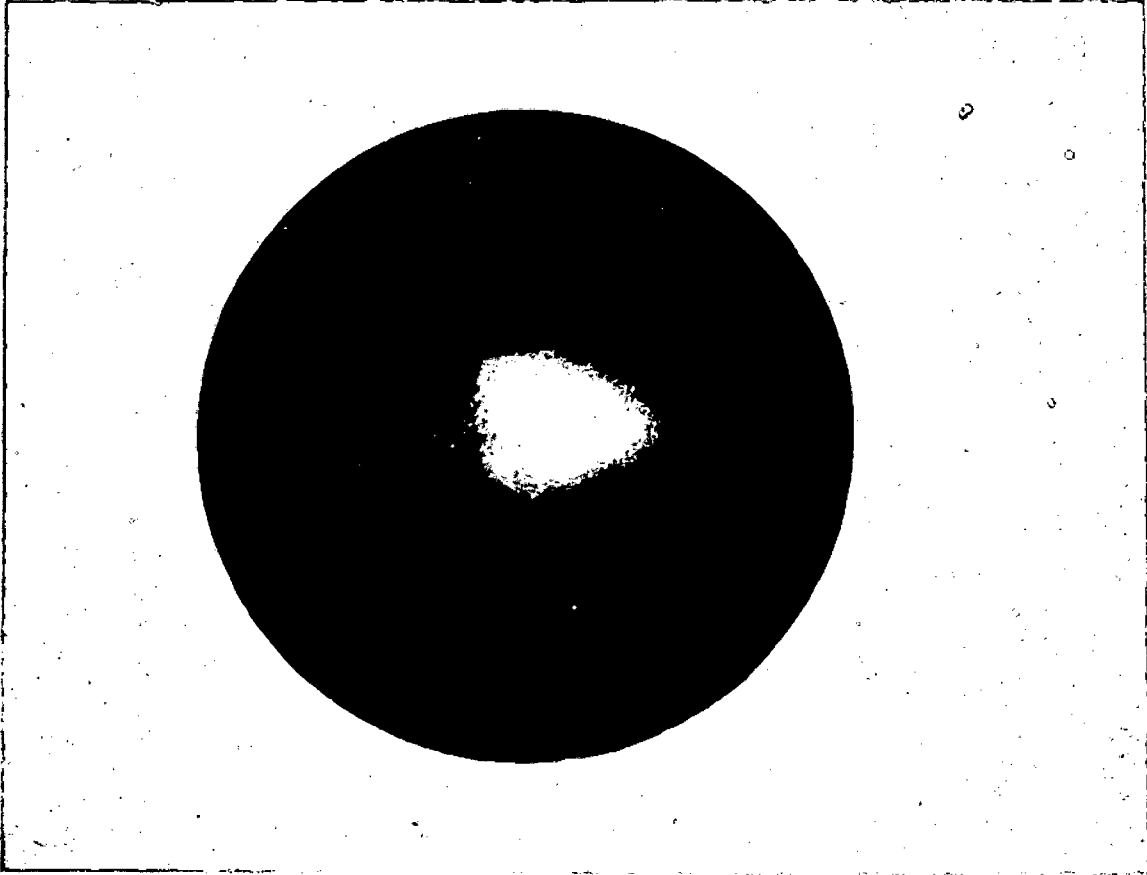
XBB 686-3754

Fig. 13



XBB 686-3756

Fig. 14



XBB 686-4014

Fig. 15

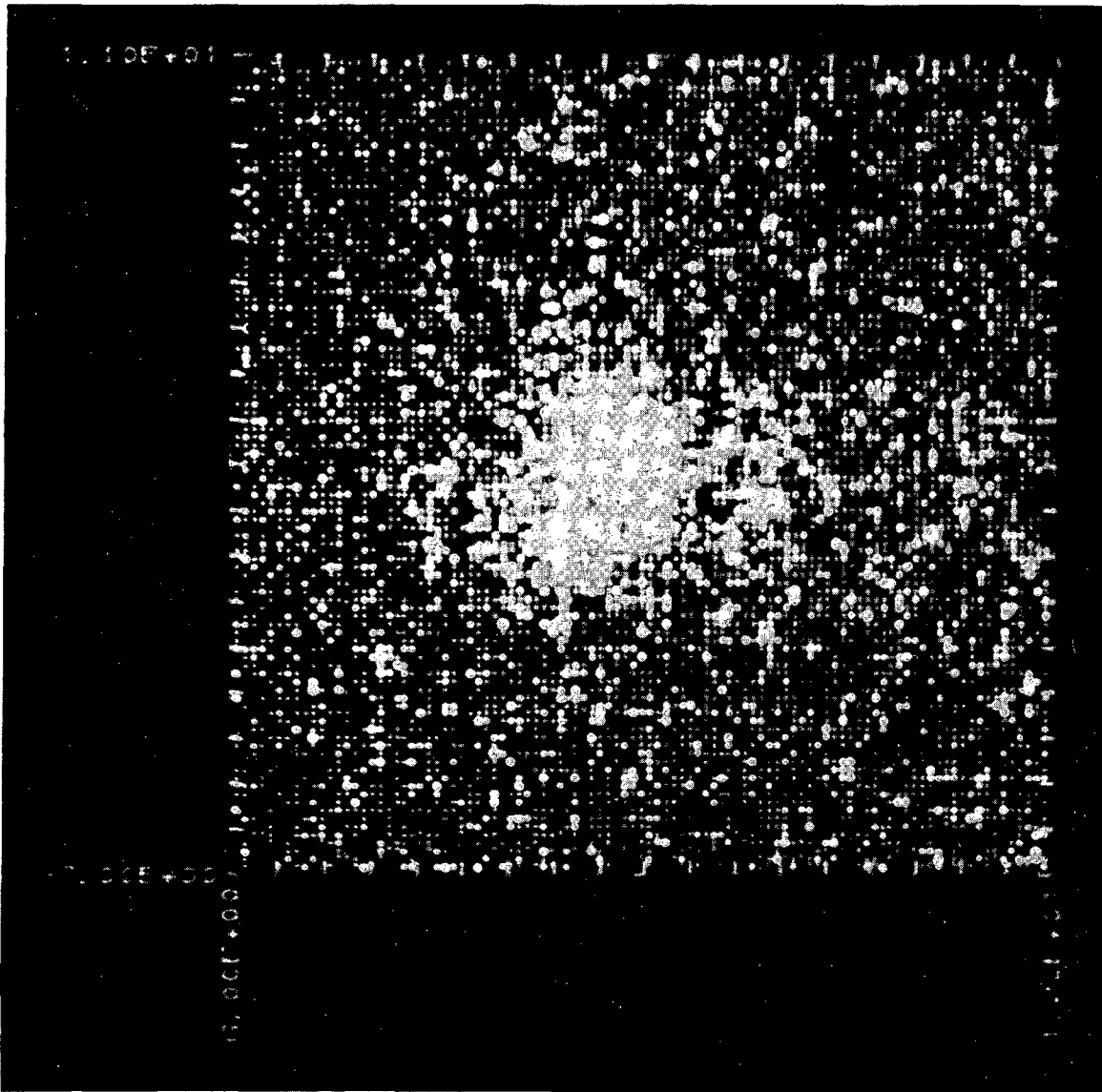
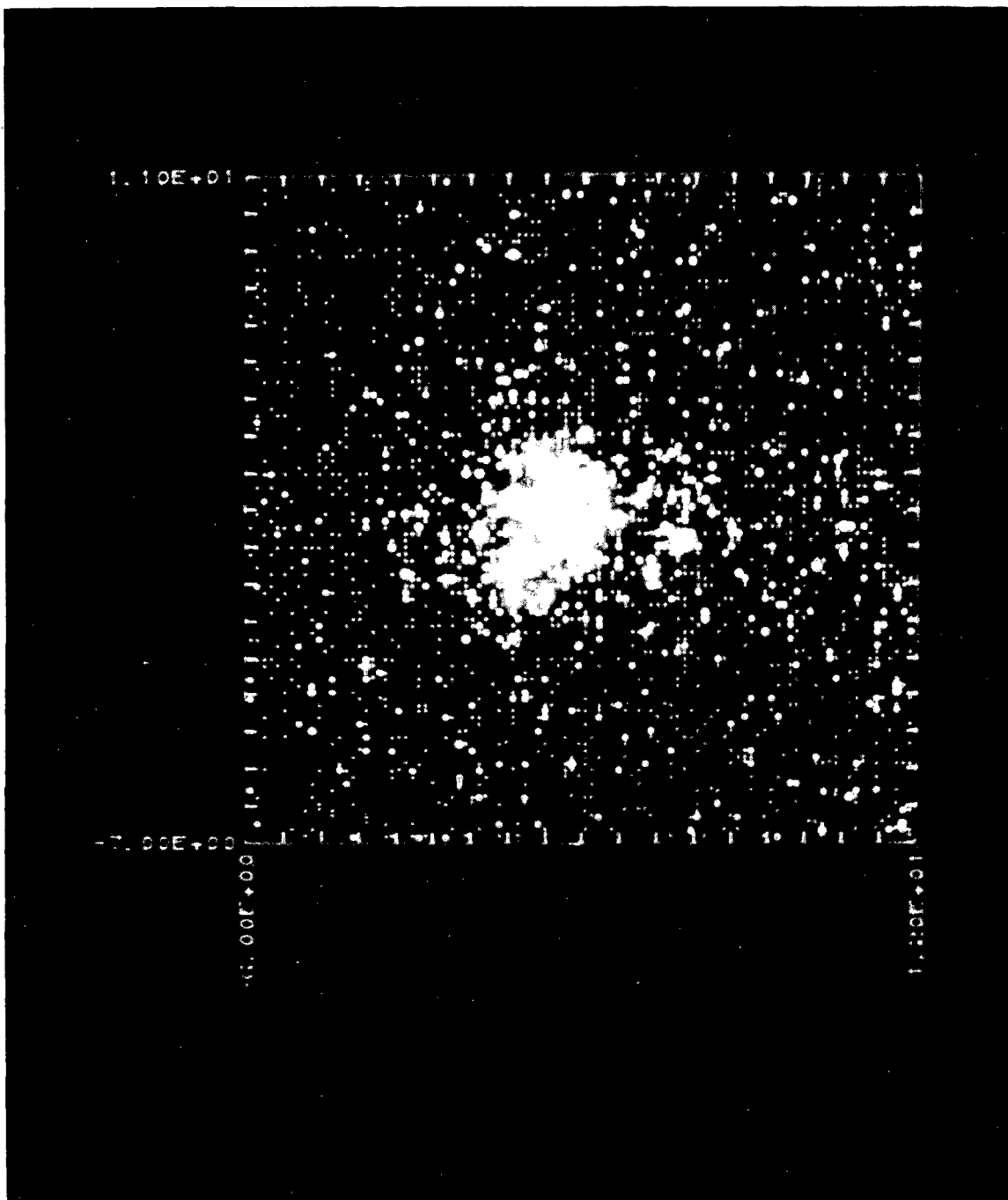


Fig. 16

XBB 686-3758



XBB 686-3760

Fig. 17

LEGAL NOTICE

This report was prepared as an account of Government sponsored work. Neither the United States, nor the Commission, nor any person acting on behalf of the Commission:

- A. Makes any warranty or representation, expressed or implied, with respect to the accuracy, completeness, or usefulness of the information contained in this report, or that the use of any information, apparatus, method, or process disclosed in this report may not infringe privately owned rights; or*
- B. Assumes any liabilities with respect to the use of, or for damages resulting from the use of any information, apparatus, method, or process disclosed in this report.*

As used in the above, "person acting on behalf of the Commission" includes any employee or contractor of the Commission, or employee of such contractor, to the extent that such employee or contractor of the Commission, or employee of such contractor prepares, disseminates, or provides access to, any information pursuant to his employment or contract with the Commission, or his employment with such contractor.

TECHNICAL INFORMATION DIVISION
LAWRENCE RADIATION LABORATORY
UNIVERSITY OF CALIFORNIA
BERKELEY, CALIFORNIA 94720